Oleuropein from olive leaf extracts and extra-virgin olive oil provides distinctive phenolic profiles and modulation of microbiota in the large intestine

Gabriele Rocchetti [a], Maria Luisa Callegari [a,*], Alice Senizza [a], Gianluca Giuberti [a], Jessica Ruzzolini [b], Annalisa Romani [c], Silvia Urciuoli [c], Chiara Nediani [b,*], Luigi Lucini [a]

[a] Department for Sustainable Food Process, Università Cattolica del Sacro Cuore, Via Emilia Parmense 84, 29122 Piacenza, Italy
[b] Department of Experimental and Clinical Biomedical Sciences "Mario Serio", University of Florence, Italy
[c] PHYTOLAB (Pharmaceutical, Cosmetic, Food Supplement, Technology and Analysis)-DiSIA, University of Florence, Via U. Schiff, 6, 50019 Sesto Fiorentino, Italy

ARTICLE INFO

ABSTRACT

The interest in the modulation of gut microbiota by polyphenols from olives and derived products is increasing. In this work, phenolic leaf extracts (PLE) were *in vitro* faecal fermented to evaluate the changes in phenolic profiles and the impact on microbiota, using a commercial extra-virgin olive oil (EVOO) as reference. The *in vitro* fermentation decreased oleuropein content in PLE, determining an increase of hydroxytyrosol and other phenolic metabolites. An increase ($p < 0.05$) of hydroxytyrosol (LogFC = 6.02; VIP score = 1.05) was also observed in fermented EVOO. Besides, PLE significantly ($p < 0.05$) changed amino acids (LogFC = 6.1) and fatty acids (LogFC = 5.9) profile of the faeces. Metagenomic sequencing revealed that *Coriobacteriaceae* at the family level, and *Collinsella* at the genus level, were the most affected by PLE fermentation. These findings support the modulation of the gut microbiota exerted by phenolics from PLE and EVOO.

1. Introduction

Olive tree leaves (*Olea europaea* L.) are used in the Mediterranean basin in traditional medicine (Abaza, Taamalli, Nsir, & Zarrouk, 2015), since their polyphenol content is higher than that in extra virgin olive oil or whole fruit (Jimenez-Lopez et al., 2020). Also, olive leaves represent a cheap raw material that green technologies can recover and exploit as a good source of high-added value bioactive compounds, mainly polyphenols, to be used in food, agronomic, nutraceutical, and biomedical applications (Peršurić, Saftic, Klisović, & Kraljević Pavelić, 2019; Romani et al., 2019).

Specifically, oleuropein (Ole) is the main phenolic in olive leaves, together with other secoiridoids derived from the tyrosol structure, followed by flavonoids, lignans, and phenolic acid derivatives (Rocchetti et al., 2020;). The phenolic composition is strictly dependent on geographical origin, type of cultivar, and tree age (Ben Mohamed et al., 2018; Ghisoni et al., 2019), while the polyphenol yield in the extracts from olive leaves is strongly influenced by the extraction method (Dobrinčić et al., 2020). Notwithstanding, the relevance of bioactive components in olive leaves and extra-virgin olive oil (EVOO) has been

strengthened by the European Food Safety Authority (EFSA) in 2011, who granted a health claim on the efficacy of olive oil phenolics (5 mg/day per 20 g of EVOO). Olive phenolics can prevent low-density lipoprotein (LDL) oxidation, the initial event of atherosclerotic plaque formation (Journal, 2011). This is of pivotal interest because, to date, it represents one of the few available claims linking a specific dosage of phenolics from foods with a health-promoting property (such as a cardiovascular risk reduction). In this regard, also cocoa flavanols have been described by EFSA as maintaining endothelium-dependent vasodilation, which contributes to normal blood flow. Overall, 200 mg of cocoa flavonols should be consumed daily to obtain the claimed effect. Regarding olives and olive oil, a large body of evidence suggests that Ole and hydroxytyrosol exert various protective effects against several pathologies such as neuro- and cardiovascular diseases, diabetes mellitus, cancer, and chronic kidney disease, likely through a putative antioxidant and anti-inflammatory activity (Nediani, Ruzzolini, Romani, & Calorini, 2019; Romani et al., 2019). In addition, Ole presents other peculiar features such as autophagy inducer (Miceli et al., 2018; Rigacci et al., 2015) and amyloid fibril growth inhibitor (Rigacci et al., 2010) and, finally, anti-cancer activity (Ruzzolini et al., 2018, 2020).

In recent years, a considerable interest in gut microbiota has grown fast due to its role in human health. Indeed, the gut microbiota has been pointed out to play a pivotal role in intestinal inflammatory disorders, obesity, autism spectrum disorders, and immune system disorders, among others (Lobionda, Sittipo, Kwon, & Kyung Lee, 2019). In addition, gut microbial metabolites may have a significant influence on host health. Once administered, polyphenols may undergo extensive transformation *via* phase I and phase II metabolism and interfere with gut microbiota. The data on the microbial change of Ole and other phenolics from EVOO or olive leaves in humans are poor, and conflicting results have been reported on the level and the forms found in different biofluids (Farràs et al., 2020; Rocchetti et al., 2020). Despite representing an excellent source of Ole and other phenolics, very little information is available on the intestinal bioaccessibility of olive leaf extracts and their impact on gut microbiota. This may be of concern, considering that phenolics need to be bioaccessible at a sufficient dose to exert their biological effects. Therefore, much attention should be paid to gut microbiota, as a metabolic system impacting host nutrition and affecting the bioavailability and bioaccessibility of phenolics via biotransformation into other active substances having potential health benefits. Mosele et al. (2014), using an *in vitro* model experiment, observed that Ole was rapidly de-glycosylated during 6 h of incubation by human faecal microbiota, becoming Ole-Aglycone. This latter was degraded into elenolic acid and hydroxytyrosol by microbial esterases, to disappear after 48 h. On the contrary, hydroxytyrosol constantly increased during the fermentation period. The same authors confirmed this finding *in vivo*, showing that the intake of phenolics-rich olive oil for three weeks significantly increased the concentration of hydroxytyrosol in the faeces in human volunteers.

Given the lack of comprehensive studies dealing with the correlation between polyphenols from olive leaf extracts and gut microbiota, our work aimed at investigating the impact of phenolic leaf extracts (PLE) on the gut microbiota. To this aim, PLE (differing for Ole enrichment level and phenolic profile) were *in vitro* digested and *in vitro* fermented. Also, we investigated the impact of these compounds on gut microbiota profile during the *in vitro* faecal fermentation process. A commercial EVOO sample was used as a reference, to highlight the biochemical processes specifically modulated by PLE phenolics.

2. Materials and methods

2.1. PLE and EVOO samples

Olea europaea L. organic green leaves (from Frantoio and Leccino cultivars) were collected in Tuscany (Vinci, Florence, Italy) and immediately processed to obtain micronized powder extracts, according to a previously described and standardized procedure (Romani et al., 2020). In this work, two different phenolic leaf extracts (PLE) were considered, namely PLE1 (total phenolic content: 383 mg/g, Ole: 298.48 mg/g) and PLE2 (total phenolic content: 219 mg/g, Ole: 189.26 mg/g) as reported in Supplementary material (supplementary table 1). The PLE1 and PLE2 samples were obtained from a blend (50:50 w/w) of olive leaves from Leccino and Frantoio cultivars, and the extraction process was previously optimized to provide a different total phenolic content (Romani et al., 2020). Both extracts were obtained through an extraction process based on the utilization of membrane purification and vacuum concentration steps, but with different nanofiltration size and fractionation times. Besides, a commercial EVOO sample (from Leccino cultivar) was acquired from a local supermarket (Piacenza, Italy) and used as a comparison. The selected EVOO sample was immediately placed in dark and cold storage (10 ± 2 °C). Prior to being used in the fermentation trial, the PLE1 was tested to exclude cytotoxicity or inflammatory activity.

2.2. Cell viability and nitric oxide (NO_2^-) assay following the addition of PLE1

Cell viability was determined in two different cell lines (namely murine macrophages RAW 264.7 and murine Aortic Endothelial Cell, MAEC) by adding PLE1 to varying concentrations for 24 h, using MTT (3-(4,5-dimethylthiazol-2-yl)-2,5-diphenyltetrazoliumbromide) tetrazolium reduction assay (Sigma Aldrich, Milan, Italy) as described in Ruzzolini et al. (2018). For nitric oxide, NO_2^- measurement was used. Cell media culture of RAW 264.7, treated with PLE1 at different concentrations in the presence or the absence of 1 µg/ml lipopolysaccharide (LPS), were then collected and transferred into a 96 well plate in the presence of 1:1 Griess (Sigma Aldrich, Milan, Italy). After 15 min of room temperature incubation, the plate was read at 540 nm using the microplate reader (Bio-Rad, Milan, Italy). The obtained absorbances were normalized on the amount of protein, and the results were expressed as a percentage of LPS positive control.

2.3. Western blot analysis for anti-inflammatory activity of PLE1

Cells were lysed and separated using electrophoresis as previously described (Ruzzolini et al., 2018). The primary antibodies were rabbit anti-iNOS (1:1000, Cell Signaling Technology, Danvers, MA, USA), rabbit anti-COX-2 (1:1000, Cell Signaling Technology, Danvers, MA, USA). The membrane was washed in *T*-PBS buffer, incubated for 1 h at room temperature with goat anti-rabbit IgG Alexa Flour 750 antibody or with goat anti-mouse IgG Alexa Fluor 680 antibody (Invitrogen, Monza, Italy), and then visualized by an Odyssey Infrared Imaging System (LI-COR® Bioscience, Lincoln, NE, USA). Mouse anti-tubulin monoclonal antibody (1:1000, Cell Signaling Technology) was used to assess the equal amount of protein loaded in each lane.

2.4. In vitro digestion and large intestine fermentation of PLE and EVOO samples

The PLE and EVOO samples were firstly subjected to a standardized static *in vitro* human gastrointestinal digestion system (Brodkorb, Egger, & Alminger, 2019; Minekus, Alminger, & Alvito, 2014). The method was scaled up for 2 g of sample. An oral digestion phase (2 min), a gastric digestion phase (120 min), and an intestinal digestion phase (120 min) at 37 °C were conducted. Simulated digestion fluids, enzyme concentrations, and *in vitro* conditions were according to Minekus et al. (2014). Enzymes (human salivary α- amylase Type IX-A; porcine pepsin P7000; pancreatin P1750 and bile salts B8631) were acquired from Sigma-Aldrich (Milan, Italy). The *in vitro* gastrointestinal digestion was run in amber bottles, and at the end of the intestinal phase, bottles containing samples were cooled on ice and centrifuged at 10,000×*g* for 15 min. The incubation was run in triplicate.

The *in vitro* large intestine fermentation was conducted on the unhydrolyzed residues (i.e., the solid pellet for PLEs and the oil phase at the top of the centrifuge tube for EVOO) following the procedure of Rocchetti et al. (2019). The method was scaled up for 50 mg of sample. Fresh faeces were collected from 6 growing pigs (31.7 ± 4.01 kg body weight; 3–5 months of age) with free access to water and fed a commercial diet devoid of antibiotics. This study used a pig faecal inoculum, considering the physiological similarity between humans and pigs in the gastrointestinal tract, digestive functions, and gastrointestinal fermentation profiles. In addition, both pigs and humans are colon fermenters, and they have a comparable composition of the colonic microbiota (Heinritz, Mosenthin, & Weiss, 2013; Roura et al., 2016).

Freshly voided faecal samples were captured after the physiological defecation, pressed in sterile, airtight plastic syringes, and kept at 39 °C. Faecal samples were used within 15 min after collection. Unhydrolyzed residues were weighed in triplicate into an amber glass bottle filled with a buffer-mineral solution (Williams, Bosch, Boer, Verstegenm, & Tamminga, 2005). The CO_2-saturated fermentation medium contained 0.05

g mL^{-1} of fresh faeces obtained by pooling equal amounts (wet weight) of faeces from each animal. Three bottles without substrate were used as control of background fermentation. Sample manipulation and incubation were done under continuous CO_2 flushing (technical grade: 5.5; from SAPIO, Monza, Italy). Bottles were carefully sealed with a rubber stopper and placed in a shaking water bath (60 rpm) at 37 °C. After 20 h of incubation, samples were immersed in ice and centrifuged at 10,000×g for 12 min. Fermented samples were then collected and stored at −4 °C for further analysis.

2.5. Untargeted metabolomic profiling by high-resolution mass spectrometry of the faecal fermented samples

In the next step, 1 mL of the fermented samples were extracted in 70% methanol (LC-MS grade, Sigma-Aldrich, Milan, Italy) acidified with 3% formic acid. Each sample was stored overnight at −18 °C and then centrifuged adopting the following conditions: 10,000×g, 15 min, and 4 °C. Finally, each aliquot was filtered using cellulose syringe-filters (0.22 μm) in dark vials for analysis.

Metabolomics and phenolic profiles were determined in the methanolic extracts by ultra-high-performance liquid chromatography (UHPLC) coupled with quadrupole-time-of-flight (QTOF) mass spectrometry, as previously described (Rocchetti et al., 2020). The database Phenol-Explorer 3.6 (Rothwell et al., 2013) and the comprehensive microbial metabolites database "MetaCyc" (Caspi et al., 2020) were used for features annotation, using a cut-off value of 5-ppm for mono-isotopic mass accuracy, and using isotopic patterns (isotopes ration and spacing) to strengthen annotations. The annotation was made according to a Level 2 of confidence (i.e., putatively annotated compounds) as set out by Cosmos standards in metabolomics (Salek, Steinbeck, Viant, Goodacre, & Dunn, 2013). Finally, the metabolites passing mass (5 ppm) and retention time (0.1 min) alignment, passing filters by frequency (being in at least 100% of replications within at least one condition), and having a peak intensity significantly different (5-folds) from the control (faeces only) were retained in the dataset.

The semi-quantification of the different phenolic compounds annotated in raw EVOO and following the *in vitro* fermentation of both PLE and EVOO samples was done according to the method previously reported by Rocchetti et al. (2020). Briefly, the polyphenols annotated were ascribed to classes and sub-classes, and then cumulative intensities were calculated. To this aim, methanolic standard solutions of individual phenolics (from pure compounds, purity > 98%, provided from Extrasynthese, Lyon, France) were injected. Sesamin (lignans), ferulic acid (hydroxycinnamic acids and other phenolic acids), luteolin (flavones and other remaining flavonoids), and tyrosol (hydroxytyrosols and phenyl-alcohol related compounds) were used as representative of their respective classes. A linear fitting (not weighed and not forced to origin) was built and used for quantitative purposes. The abundance for each phenolic class or single compound was expressed as mg equivalents/kg (n = 5).

2.6. Characterization of bacteria populations

Total DNA was extracted using the FastPrep®-24 Instrument with the FastDNA® Spin Kit for Soil (MP Biomedicals, Eschwege, Germany) from each sample collected (Rocchetti et al., 2019), following the supplied protocol. The DNA quality was assessed using agarose gel electrophoresis, whereas the genomic DNA concentration was determined using Qubit dsDNA HS fluorescence assay (Life Technologies, Carlsbad, California, USA). The V3-V4 region of the bacterial 16S rRNA gene was amplified using primers Pro341F and Pro805R (Takahashi, Tomita, Nishioka, Hisada, & Nishijima, 2014). A specific seven-base long tag was added to forward and reverse primers to achieve multiplexing of samples within a single sequencing run and to attribute sequences to samples in bioinformatics analysis. Amplification was carried out following the PCR protocol described by Rocchetti et al. (2019). PCR products

were quantified using Qubit dsDNA HS fluorescence assay (Life Technologies, Carlsbad, California, USA), and agarose gel electrophoresis was used to check the quality. To obtain a pool of amplicons, the PCR products were combined in equimolar concentration, and the pool was finally purified using DNA Clean & Concentrator™-5 Kit (Zymo Research, Irvine, CA, USA).

Sequencing was performed by Fasteris SA (Geneva, Switzerland) on the MiSeq system (Illumina) with 2 × 300 bp paired-end reads. Trimmomatic (version 0.32) (Bolger, Lohse, & Usadel, 2014) was used for the barcode sorting to remove the adapter sequence from the reads. During this process, a sliding window trimming was performed and reads showing a length shorter than 60 bases were filtered by dropping reads and then excluded from the analysis. The alignment is done using the mapping software Burrows-Wheeler Alignment version 0.7.5 (http://bio-bwa.sourceforge.net/), and the overlapped reads were mapped against the SILVA database (Version SSURef_NR99_138_tax_silva_DNA. fasta). Sequences were clustered into OTUs using the SAM tools package (Miragoli et al., 2021). Raw Illumina sequencing files were deposited in the European Nucleotide Archive (ENA) database and are available under accession number PRJEB40736.

2.7. Multivariate statistics and pathway analysis

The statistical analysis of cytotoxic and inflammatory data was performed using ANOVA and Dunnett's multiple comparison test, and p ≤ 0.05 was considered statistically significant.

The metabolomic dataset was elaborated using the software Mass Profiler Professional (Agilent Technologies) (Rocchetti et al., 2019). The abundance of metabolites was normalized at the 75th percentile and median centered. Volcano Plot analysis was next carried out to identify differential metabolites, by combining Fold-Change (FC) analysis (cut-off = 1.2) and ANOVA (p < 0.01, Bonferroni multiple testing correction). After that, unsupervised Hierarchical Cluster Analysis (HCA) was used to investigate similarities/dissimilarities across treatments and samples. The metabolomics dataset (resulting from the annotation against MetaCyc Database) was then loaded into SIMCA 13 (Umetrics, Malmo, Sweden) for the supervised OPLS-DA analysis. Confidence limits of 95% and 99% were used to check for the presence of outliers (suspect and strong outliers, respectively, according to Hotelling's T2 approach), while cross-validation (CV-ANOVA, p < 0.01) and a permutation test (N = 200) to validate and exclude overfitting, respectively, were also carried out. The goodness-of-fit and prediction ability of the OPLS-DA model (i.e., R^2Y and Q^2Y, respectively) were also checked. The VIP (variable importance in projection) selection method was carried out to identify discriminant metabolites. Generally, according to software recommendations (Umetrics, Malmo, Sweden), VIP markers>1 were considered the most meaningful in the prediction model. Also, a Venn diagram was done to check the exclusive metabolites significantly characterizing the metabolomic changes during *in vitro* faecal fermentation, considering both PLEs and EVOO. Finally, a smart table was created using a targeted list of compounds obtained considering VIP markers having FC values > 1.2 and loaded into the omics-dashboard (Paley et al., 2017) of the online tool to point out the microbial pathways and processes most affected by the *in vitro* faecal fermentation of the different samples.

Regarding the metagenomic data, the statistical analysis of the sequences was done using the MicrobiomeAnalyst tool (Chong et al., 2020). In particular, the alpha diversity was calculated based on Chao, observed species, Simpson, and Shannon metrics, thus evaluating the significant differences using a *t*-test ANOVA. Additionally, the beta diversity was calculated according to the Bray–Curtis index using a PERMANOVA statistic method, while the community beta diversity across samples was assessed through a Principal coordinate analysis (PCoA) plot. Also, the same MicrobiomeAnalyst tool (Chong et al., 2020) was used for the Random Forest analysis. Significant differences in the taxa abundance between the different sample groups were identified using

the edgeR algorithm (adjusted *p*-value cut-off = 0.05).

3. Results and discussion

3.1. PLE cytotoxicity and anti-inflammatory activity

In this work, we firstly tested the potential toxicity of the leaf extract with the highest oleuropein content (PLE1) before subjecting the PLEs to *in vitro* simulated gastrointestinal processes, since the absence of toxicity is a prerequisite to evaluate further potential benefits. The toxicity was checked on two different cell lines, namely murine macrophages RAW 264.7 and Murine Aortic Endothelial Cell (MAEC). The cell vitality was evaluated after PLE1 treatment for 24 h by the MTT assay.

A different sensitivity could be found in the two cell lines at the highest concentrations of PLE1. In detail, PLE1 significantly decreased cell vitality in MAEC already at 160 μM, whereas no significant reduction was observed in RAW cells (Supplementary Fig. 1). Inflammation represents a "common ground" of multi-factorial diseases, playing a crucial role in promoting many disabling pathologies and non-communicable diseases. Macrophages are the main factors in the inflammatory response, so we used these cells and LPS-treated RAW 264.7 cells as a model to study the anti-inflammatory effect of PLE1. The overproduction of NO_2^- by inducible nitric oxide synthase (iNOS) is a representative inflammatory reaction, and Cyclooxygenase-2 (COX2) is another inflammatory marker associated with an upregulation of proinflammatory substances, such as prostaglandins. We found that the NO_2^- level in cell media culture was reduced by PLE1 treatment for 24 h in a dose-dependent manner. Interestingly, this decrease was significant already at a physiologically relevant concentration (11–22 μg/mL, 20–40 μM). The reduction in NO_2^- production was due to the down-regulation of iNOS content (as shown in Supplementary Fig. 2), also observed at 40 μM, whereas PLE1 exerted on COX-2 a similar but not significant effect. These data indicated that PLE1 decreased LPS-induced NO_2^- production dose-dependently by downregulating iNOS, which is closely associated with nitric oxide synthesis. This result encourages the use of this leaf extract containing a high content of oleuropein, which might represent a potential anti-inflammatory nutraceutical source.

3.2. Transformation of Ole during in vitro faecal fermentation process

Thereafter, both the PLE extracts and EVOO samples were subjected to *in vitro* gastrointestinal digestion and fermentation to investigate the modifications of its main compound, respectively Ole and Ole aglycone. Overall, untargeted metabolomics based on UHPLC-QTOF mass spectrometry allowed us to comprehensively depict the main metabolites arising from the transformation of Ole via the phenyl alcohol pathway. According to Mosele et al. (2014), few studies have focused on the colonic pathway of these phenolic compounds, with most of the available literature focusing on flavonoids and other classes such as lignans and phenolic acids. We found an extensive transformation of Ole under our experimental conditions, following the combined gastrointestinal digestion and 20 h *in vitro* fermentation. Overall, a marked reduction of Ole could be observed for both PLE1 and PLE2 (Supplementary table 1), thus indicating a strong impact of the digestion and fermentation processes on this compound. This trend was in accordance with the data previously obtained by González et al. (2019), demonstrating that the encapsulation of an olive leaf extract with sodium alginate by spray-drying allowed the protection of Ole under gastric conditions and its controlled release at intestinal conditions, thus reaching higher bioaccessibility and potential bioavailability values. In this regard, these authors have observed the most increased degradation for Ole already during the first 10 min of gastric digestion, leading to the simultaneous formation of both hydroxytyrosol and Ole-aglycone. Consistently, Ole has been reported to undergo non-enzymatic hydrolysis in gastric conditions, giving hydroxytyrosol (Martín-Vertedor, Garrido, Pariente, Espino, & Delgado-Adámez, 2016). The β-glycosidic bond of Ole may be

further cleaved, releasing glucose and its aglycone (Carrera-González, Ramírez-Expósito, Mayas, & Martínez-Martos, 2013). According to Carrera-González et al. (2013), Ole may be degraded by two lipases in the intestine, leading to the formation of hydroxytyrosol and oleoside-11-methyl ester, from which oleoside and methanol are derived. After intestinal digestion, the intact Ole may be fermented in the colon, giving hydroxytyrosol as an end-fermentation product, probably due to a beta-glycosidase hydrolytic activity.

The modifications of the phenyl alcohol pathways observed in this work, related to both PLE1 and PLE2, are represented in Fig. 1. After a 20-hours incubation step, there was a high production of 3,4-dihydroxyphenyl propionic acid, likely deriving from Ole (on average: 0.75 mg/g). This phenolic metabolite represents an important and common faecal metabolite belonging to other pathways, such as phenyl acids and benzoic acids (Mosele et al., 2014). On the other hand, as reviewed by Farràs et al. (2020), Ole can be converted into hydroxytyrosol by several bacterial strains, such as *Lactobacillus*, *Bifidobacteria*, and *Enterococcus*. As shown in Fig. 1, the deglycosylation and hydrolysis of Ole led to the appearance of an average content of 0.43 mg/g of hydroxytyrosol. In contrast, further oxidation and dehydroxylation reactions led to two very important and common large intestinal metabolites, namely 3,4-dihydroxyphenylacetic acid (average content: 0.16 mg/g) and 4-hydroxyphenylacetic acid (average content: 0.07 mg/g). Interestingly, the untargeted UHPLC-QTOF analysis showed no elenolic acid at 20-hours of incubation. This latter (described in the literature as particularly unstable; Bellumori et al., 2019) is another product of the deglycosylation and hydrolysis of oleuropein. Regarding the commercial EVOO under investigation, its phenolic profile was characterized by 24 compounds, with a great abundance of tyrosol-derivatives, followed by phenolic acids, lignans, and flavonoids (Supplementary table 1). Besides, we found semi-quantitative contents of 13.55 mg/kg for Ole-aglycone and 0.11 mg/kg for Ole on the raw sample. Interestingly, the EVOO sample was also abundant in oleacein (69.05 mg/kg) and oleocanthal (21.17 mg/kg), two compounds recognized as potential precursors of hydroxytyrosol. Accordingly, after 20 h of *in vitro* faecal fermentation, Ole and its aglycone, together with oleacein and oleocanthal were not detected, with a corresponding increase of hydroxytyrosol (18.42 mg/kg; Supplementary table 1).

Considering the complex colonic pathway previously described, it is possible to conclude that the microbial transformation of PLE1 and PLE2 led to the accumulation of metabolites produced during the *in vitro* digestion step (such as Ole-aglycone and hydroxytyrosol) and likely further processed by the large intestinal microbiota. In this regard, these initial metabolites reaching the large intestine were processed further by the microbiota, leading to the accumulation of final catabolites common to different phenolic sub-group (such as the phenolic acids pathway). This hypothesis is in accordance with the findings previously reported in another of our research work (Rocchetti et al., 2020), showing that Ole-aglycone was converted to hydroxytyrosol during the *in vitro* simulated digestion process (considering both gastric and pancreatic phases), moving from an average value of 1.3 (before the *in vitro* digestion) up to 9.7 mg equivalents/kg during the pancreatic step. As proposed in the literature, the increase in hydroxytyrosol might result from the combined effect of lipase(s) activity and acidic conditions during the digestion process. Therefore, in this work, we demonstrated that *ad-hoc* carrier conditions (such as those based on encapsulation technologies) are strongly advised to prevent Ole transformation before its arrival to the large intestine, where it can be further processed into lower-molecular-weight phenolic metabolites.

3.3. Chemical changes during the in vitro faecal fermentation of both PLE and EVOO

In the second part of this work, we used an untargeted metabolomic approach exploiting the comprehensive database MetaCyc for annotation purposes to investigate the shift in faecal metabolome following
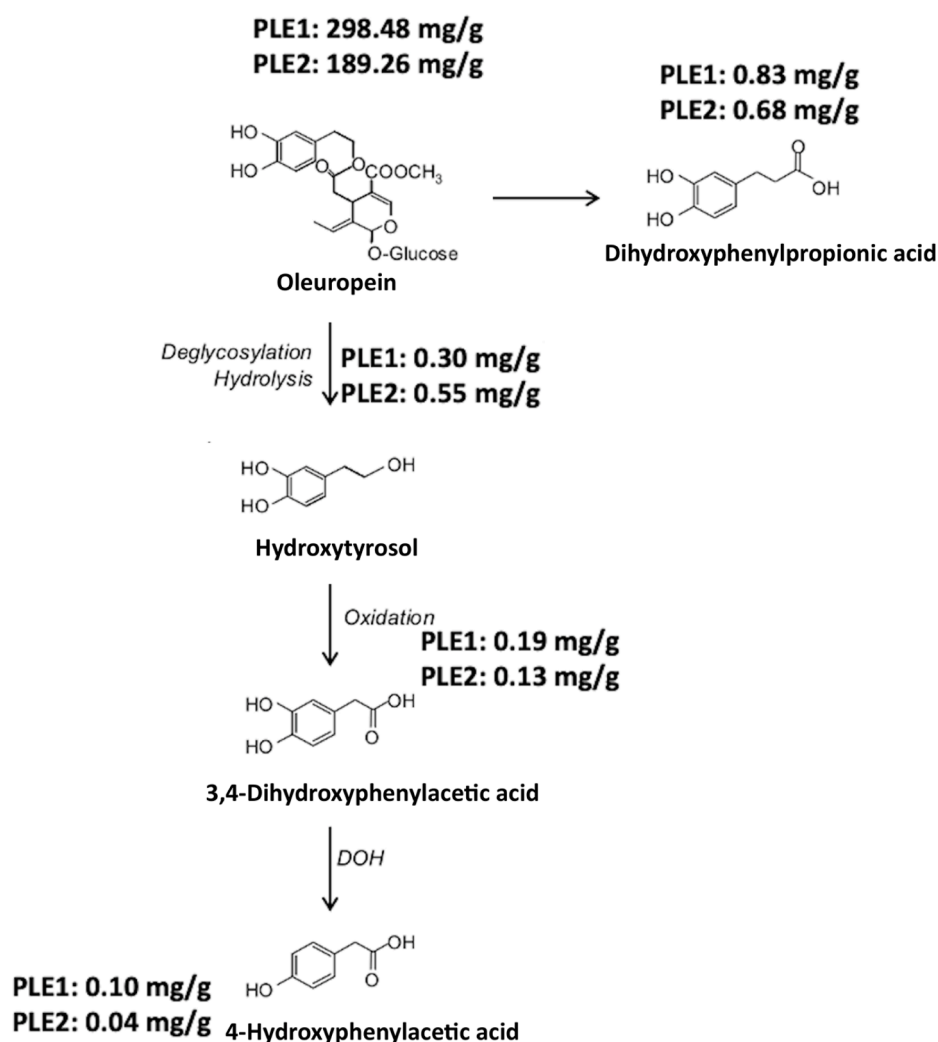
PLE1: 298.48 mg/g
PLE2: 189.26 mg/g

PLE1: 0.83 mg/g
PLE2: 0.68 mg/g

Oleuropein

Dihydroxyphenylpropionic acid

Deglycosylation Hydrolysis PLE1: 0.30 mg/g
PLE2: 0.55 mg/g

Hydroxytyrosol

Oxidation PLE1: 0.19 mg/g
PLE2: 0.13 mg/g

3,4-Dihydroxyphenylacetic acid

DOH

PLE1: 0.10 mg/g
PLE2: 0.04 mg/g **4-Hydroxyphenylacetic acid**

Fig. 1. Phenyl alcohol pathway following the *in vitro* gastrointestinal digestion and faecal fermentation of PLE1 and PLE2.

PLE and EVOO intake. Indeed, such changes in metabolomic signatures may reflect the modulation of the microbial community in the large intestine. A total number of 5359 metabolites was putatively annotated; the detailed list reporting each metabolite with individual abundances, together with composite mass spectra (mass & abundance combinations) can be found in Supplementary table 1.

A multivariate statistical approach based on both unsupervised and supervised tools was used to reduce the data complexity and extrapolate the metabolomic differences induced by PLE and EVOO. Firstly, we inspected the outputs provided by the principal component analysis (PCA score plot) and the hierarchical clustering analysis (fold change-based heat map). As can be observed from the PCA score plot (Supplementary Fig. 3), the two principal components were able to explain a very high percentage (71.75%) of the total variability, thus revealing a clear impact of the matrix (either PLE or EVOO) on the faecal metabolome detected by UHPLC-QTOF mass spectrometry. In this regard, the PC1 clearly described the differences between the EVOO and the PLE samples, while the PC2 depicted the metabolomic differences existing between the faecal samples incubated with PLE1 and PLE2 samples. This latter aspect is of particular interest, considering that PLE1 and PLE2 substantially differed on the initial abundance of Ole and its aglycone. The heat map provided the same information resulting from the hierarchical clustering analysis (Fig. 2). In this regard, the two PLE samples were included in the same clusters, whilst the EVOO sample was found to cluster with the fermentation blank, thus showing a hierarchically lower ability of EVOO to shift the faecal metabolome and/or to

modulate the large intestine microbiota. Besides, it was evident from Fig. 2 that PLE samples were characterized by exclusive clusters of up-accumulated metabolites, thus justifying the discrimination on the second principal component revealed by the PCA score plot.

A supervised statistical approach based on OPLS-DA was then used to extrapolate the most discriminant compounds, accounting for the differences between faecal fermented PLE *vs.* EVOO samples. As shown in Fig. 3, the model separated the different treatments, thus confirming the output observed by unsupervised statistical approaches. Interestingly, the model was characterized by adequate goodness of fit ($R^2X = 0.801$; $R^2Y = 0.992$) and goodness of prediction ($Q^2 = 0.860$). The model was cross-validated by using a CV-ANOVA (p-value $< 4.2 \times 10^{-18}$) and outliers excluded by the Hotelling's *T*-squared distribution (Supplementary table 1). Also, the overfitting of the model was excluded by checking the permutation plot (number of random permutations = 200; Supplementary table 1). The VIP selection method was then used to extrapolate the most discriminant compounds allowing the separation observed in Fig. 3. In our experimental conditions, 2490 metabolites were characterized by a VIP score > 1, corresponding to 1338 unique molecular structures. Therefore, to reduce the data complexity, we used a Venn diagram reporting only up accumulated and statistically significant metabolites. As reported in Fig. 4, the Venn diagram revealed that the *in vitro* faecal fermentation of PLE1 resulted in the exclusive up-accumulation of 344 metabolites, while PLE2 and EVOO provided a lower number of compounds (274 and 221, respectively). Interestingly, 10.9% of these discriminant and significant metabolites were shared
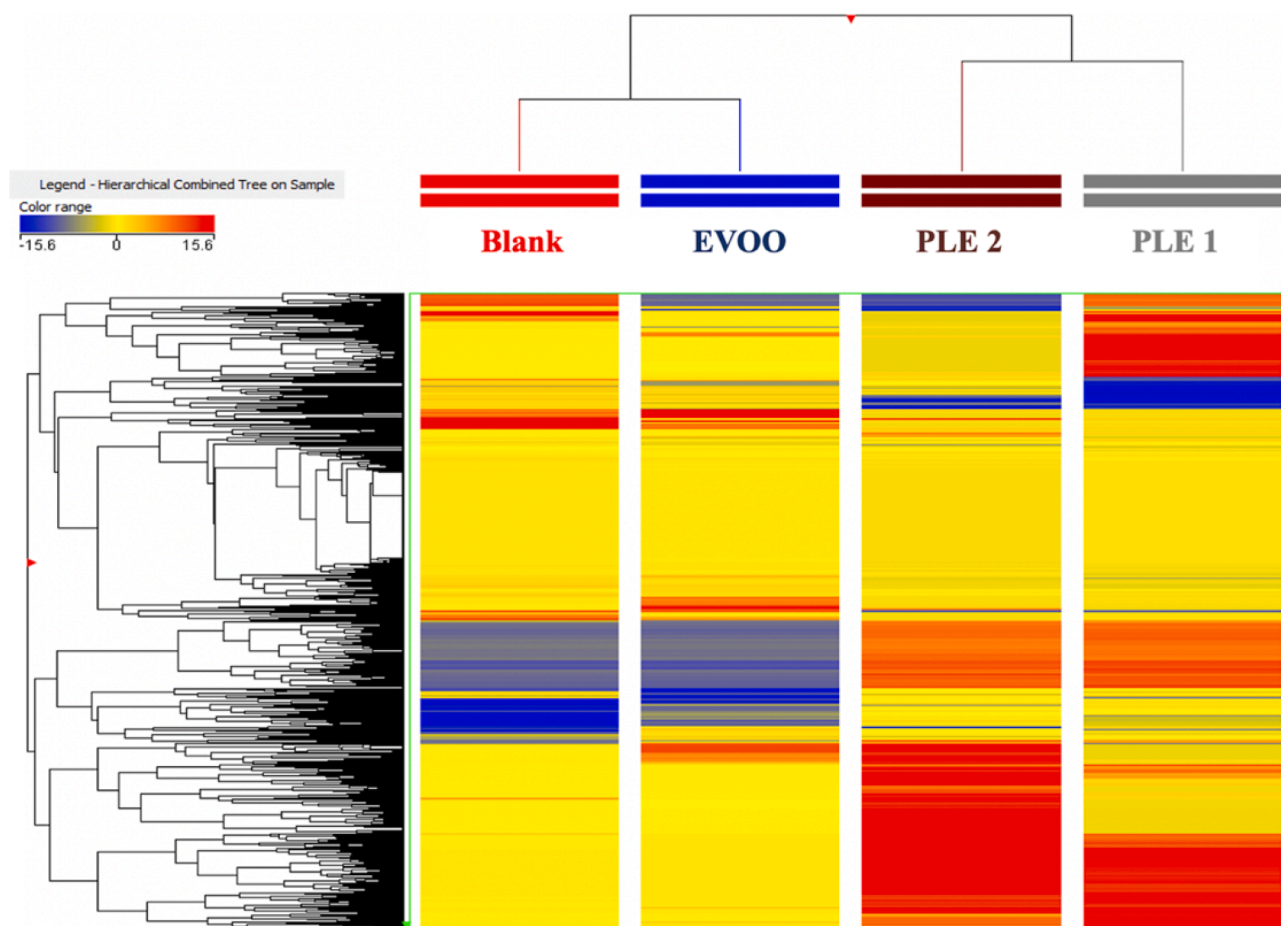
Fig. 2. Unsupervised hierarchical clustering considering the faecal metabolomic profile following the incubation with EVOO, PLE1, and PLE2 samples.
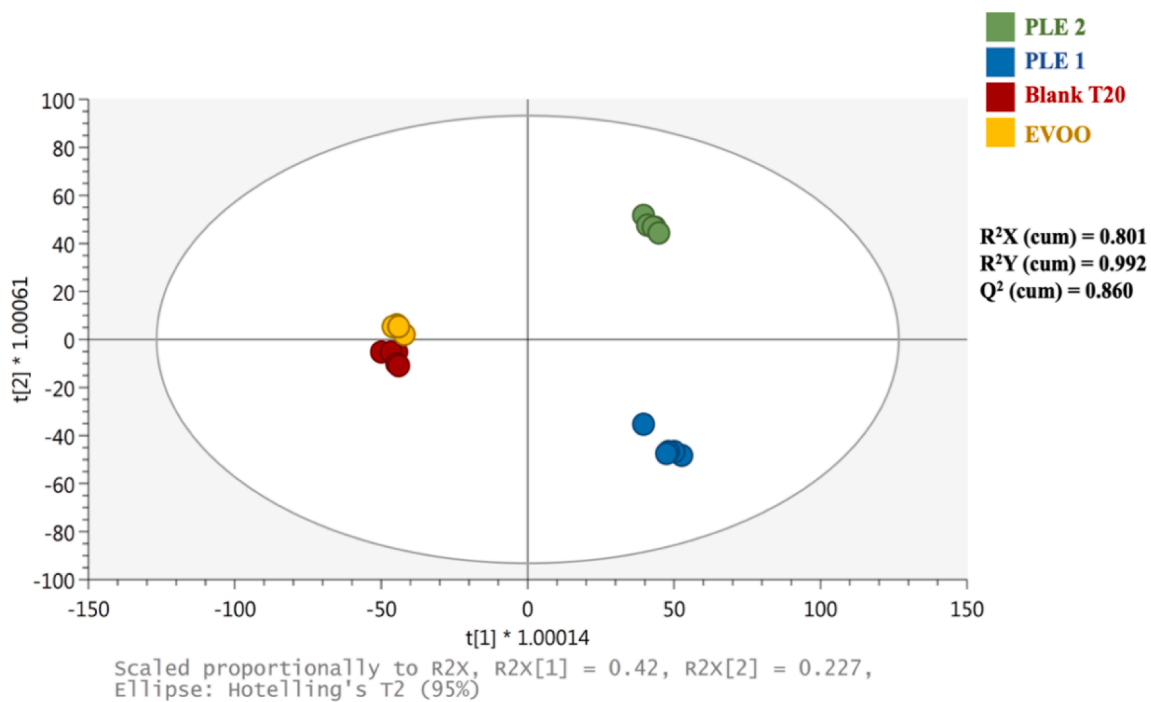

Fig. 3. Supervised OPLS-DA score plot considering the faecal metabolomic profile following the incubation with EVOO, PLE1, and PLE2 samples.
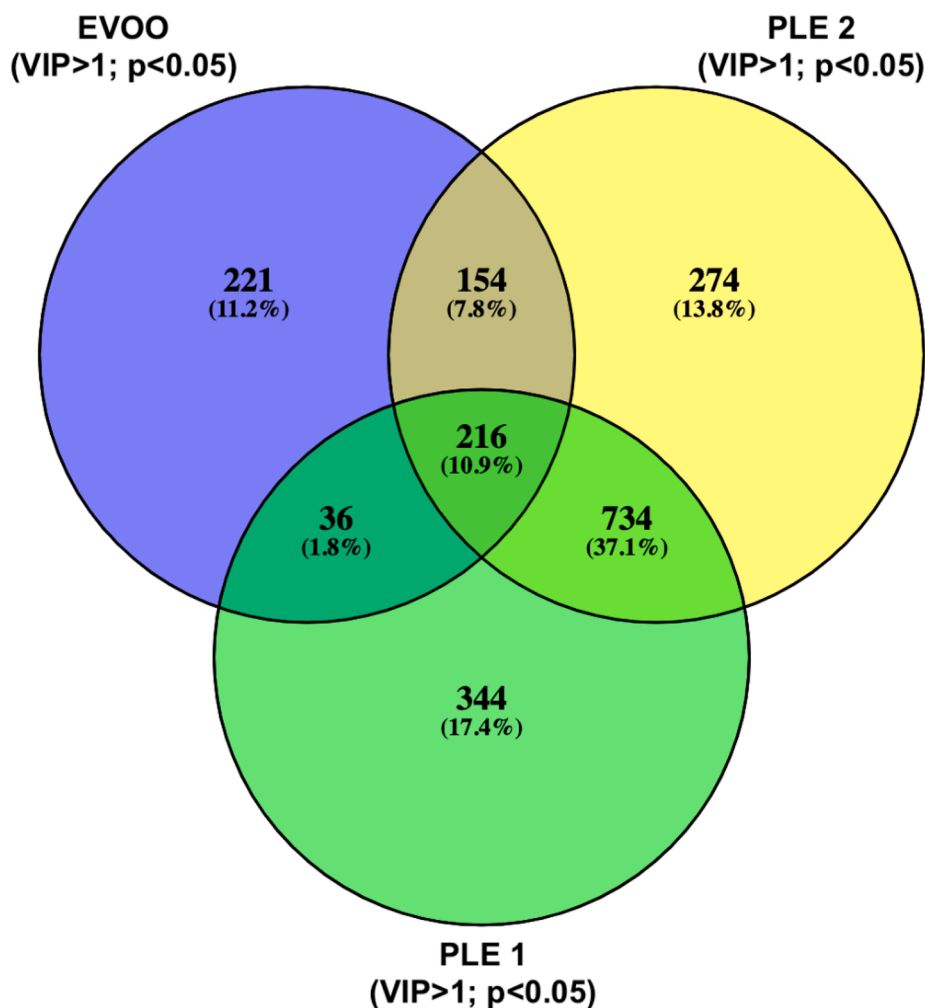
Fig. 4. Venn diagram considering the significant and discriminant compounds (annotated by MetaCyc database) arising following the *in vitro* faecal fermentation of EVOO, PLE1, and PLE2 samples.

between the EVOO and PLEs samples, while PLE1 and PLE2 shared the 37.1% (i.e., 734 compounds) of some up-accumulated discriminant metabolites. A comprehensive list reporting these exclusive and common metabolites can be found as Supplementary table 1, together with their VIP scores and LogFC values *vs.* the faecal fermentation blank. Finally, the metabolic perturbations induced by the fermentation of EVOO and PLE extracts were computationally predicted by running the relevant features (i.e., FC > 1.2 and VIP score > 1) in the Pathway tools software. Table 1 reports the main biosynthetic pathways highlighted, together with the average Log Fold Change (FC) values for each comparison. Overall, the pathway analysis confirmed a marked impact of PLE in fermented samples metabolic profile, determining an up-accumulation of amino acids (average LogFC = 6.1) and fatty acids (average LogFC = 5.9) compared to blank. As a general consideration, the fermentation of PLE extracts shifted the microbial biosynthetic metabolism in a higher magnitude when compared with the EVOO sample.

According to literature (Neis, Dejong, & Rensen, 2015), amino acids can be either utilized for the synthesis of bacterial cell components or catabolized through different pathways. Accordingly, our findings showed positive LogFC values for the degradation of the amino acids and higher when considering the fermented PLEs (Table 1). This higher rate of bacterial protein fermentation has been related to high pH and low carbohydrate availability in the large intestine. The preferred amino acid substrates of colonic bacteria include lysine, arginine, glycine, leucine, valine, and isoleucine, resulting in a complex mixture of

Table 1

Biosynthetic and degradation pathways considering the *in vitro* fermentation of EVOO, PLE1, and PLE2 samples, as resulted by Pathway Tools Omics Dashboard for MetaCyc. Each main pathway is provided together with the average Log2 Fold Change value (LogFC) *vs* the fermentation blank (i.e., faeces only). ns = not significant.

Class	Pathway	LogFC average [EVOO *vs* Blank]	LogFC average [PLE2 *vs* Blank]	LogFC average [PLE1 *vs* Blank]
Amino acids	Biosynthesis	−0.38	6.23	5.92
	Degradation	0.67	3.07	2.04
Nucleosides and nucleotides	Biosynthesis	ns	3.13	−1.75
	Degradation	ns	1.01	−3.01
Fatty acids and lipids	Biosynthesis	1.48	5.86	5.90
	Degradation	2.40	5.50	4.10
Amines and polyamines	Biosynthesis	1.40	6.60	5.90
	Degradation	2.42	1.58	1.25
Carbohydrates	Biosynthesis	−0.80	2.40	0.10
	Degradation	1.48	4.04	1.96
Secondary metabolites	Biosynthesis	−1.02	4.24	5.79
	Degradation	0.55	4.30	5.01

metabolic end-products including short-chain fatty acids and branched-chain fatty acids. These bacterial metabolites have been reported to influence epithelial physiology and modulate both the host's mucosal immune system and bacterial gene expression, leading to the production of enzymes involved in amino acid metabolism (Neis et al., 2015). Besides the utilization of amino acids, bacteria play an essential role in producing amino acids through *de novo* biosynthesis. However, less information is available in the literature regarding a potential association between the fermentation of phenolic-rich sources and a *de novo* biosynthesis of amino acids by gut microbiota (Neis et al., 2015).

Moreover, the microbial metabolism of amino acids can also give rise to biogenic amines. In our experimental conditions, we found a strong up-accumulation of amines and polyamines (Table 1) and particularly marked (LogFC = 6.60) following the fermentation of the PLE2 sample (Table 1). The decarboxylation of amino acids produces biogenic amines by the resident microbiota (Fernández-Reina, Urdiales, & Sánchez-Jiménez, 2018). Indeed, such an increase may result from the static *in vitro* fermentation static conditions we used, as proposed by Kim and Hur (2018).

3.4. Microbial profile during the in vitro large intestine fermentation

In this work, the number of total reads obtained in the samples collected after the *in vitro* faecal fermentation process was 273,149, with an average count for the sample of 22,762. The relative abundance at the phylum and family level are shown in Supplementary Fig. 4 (A and B). The comparison between the different sample groups revealed a significant reduction in the relative abundance of Bacteroidota phylum in PLE1 (FDR = 0.035), PLE2 (FDR = 0.007), and EVOO (FDR = 0.044) samples compared to a blank (faeces only). At the family and genus level, no statistical differences were detected. Besides, at the family level, the comparison between EVOO and PLE1 groups revealed a significant increase of *Coriobacteriaceae* (FDR = 0.013) in samples where PLEs were added. At the genus level, *Collinsella*, which belongs to this family, was the more represented (FDR = 0.028) in PLE1 samples. Regarding the comparison between EVOO and PLE2 samples, significant differences were detected at the phylum level. In PLE2 samples, Firmicutes (FDR = 0.033) were less abundant whereas Proteobacteria (FDR = 0.033) and Bacteroidota (FDR = 0.045) were higher compared to EVOO. Finally, considering PLE2 and PLE1 samples, a higher abundance of *Eggerthellaceae* (FDR = 0.018) was detected in PLE2 microbiota
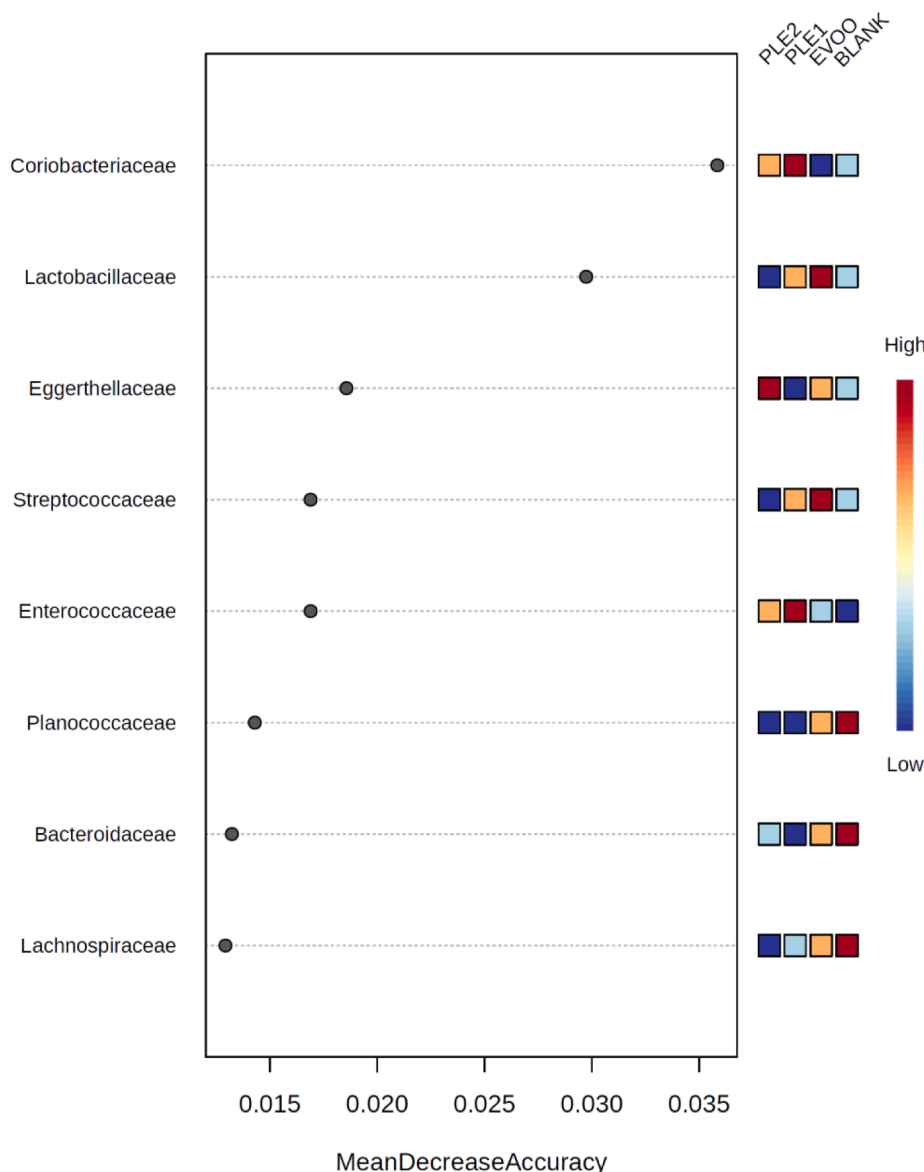

Fig. 5. Random Forest analysis revealing the most discriminant families following the *in vitro* faecal fermentation process of PLE1, PLE2, and EVOO sample.

compared to PLE1. Among this family, the *Eggerthella* genus (FDR = 0.037) was more abundant in PLE2 than PLE1.

The Random Forest analysis revealed that *Coriobacteriaceae*, *Lactobacillaceae*, and *Eggerthellaceae* were the most discriminant families (Fig. 5). Interestingly, high *Coriobacteriaceae* content was found to characterize the PLE1 samples, while *Lactobacillaceae* and *Eggerthellaceae* resulted in being more abundant in EVOO and PLE2 samples, respectively. Coriobacteriaceae is a family within the order Coriobacteriales (phylum Actinobacteria), including 30 species belonging to 14 genera (Clavel, Lepage, & Charrier, 2014). These bacteria are normal dwellers of mammalian body habitats such as the oral cavity, the gastrointestinal tract, and the genital tract. In the gut, *Coriobacteriaceae* carry out functions of importance, such as the conversion of bile salts and steroids as well as the activation of dietary polyphenols. One of the most peculiar enzymatic properties of *Coriobacteriaceae* is the conversion of food polyphenols, especially the activation of the isoflavone daidzein to the bioactive metabolite equol, together with the activation of dietary lignans to the enterolignans enterolactone and enterodiol, through deglycosylation, reduction, demethylation, dehydroxylation, and dehydrogenation reactions (Clavel et al., 2014). Accordingly, in our experimental conditions, we found a strong down-accumulation of daidzein derivatives (i.e., 3R-2′-hydroxydihydrodaidzein; VIP score = 1.02) with a corresponding significant increase of equol 4′-sulfate (VIP score = 1.05) following a 20-hours *in vitro* faecal fermentation of the PLE samples (Supplementary table 1). Also, *Eggerthella lenta* was shown to reductively cleave the heterocyclic C-ring of the flavanols epicatechin and catechin (Clavel et al., 2014). As reviewed by Rodríguez-Daza et al. (2021), the prebiotic action of phenolic compounds on the gut microbiota may directly stem from the activation of polyphenols-associated enzymes, such as tannase, quercetinase, gallate decarboxylase, esterase, and phenolic acid decarboxylase enzymes. Such activity leads to both the generation of bioaccessible phenolic metabolites and microbial cross-feeding interactions in the gut. Also, phenolic-rich powders (such as those analyzed in this work) and high molecular-weight polymeric fractions have been previously reported to significantly increase the proportion of *Eggerthellaceae* and *Coriobacteriaceae* families in the gut microbiota of humans and animals, two families displaying unique ability to break down polyphenols and transform them into trophic growth factors (Rodríguez-Daza et al., 2021). Additionally, the results detected in EVOO samples are in strict agreement with those previously described by Farràs et al. (2020), outlining those strains belonging to *Lactobacillus*, *Bifidobacterium*, and *Enterococcus* species showed the *in vitro* capability to hydrolyze oleuropein to form hydroxytyrosol (Santos, Piccirillo, Castro, Kalogerakis, & Pintado, 2012). Other authors described a different modulation on the gut microbiota due to EVOO consumption, mainly depending on the *Lactobacillus* species considered (Liu, Wang, Ma, & Wen, 2019; Prieto et al., 2018).

4. Conclusions

The present work evaluated the ability of olive leaves extracts to provide phenolic compounds in the large intestine and to modulate the microbiota, using untargeted metabolomics together with *in vitro* digestion and fermentation. As expected, the *in vitro* processes decreased oleuropein content and determined a concurrent increase of hydroxytyrosol. Moreover, the catabolic processes of phenolics in PLE leaded to the increase in small molecular weight phenolics such as homovanillic acid, 3,4-dihydroxyphenylacetic acid, and 4-hydroxyphenylacetic acid. Interestingly PLE and EVOO produced distinctive discriminant metabolites and differently shaped metabolite profiles in faeces. Similarly, metagenomic sequencing of microbiota provided differences in modulation at both family and genus level, between PLE and EVOO. Together with supporting a potential implementation in functional foods, these distinctive effects between PLE and EVOO indicate that we cannot generalize about the effect(s) of phenolic compounds in the large intestine and that *ad hoc* studies are rather necessary.

Appendix A. Supplementary data

Supplementary data to this article can be found online at https://doi.org/10.1016/j.foodchem.2022.132187.

References

Abaza, L., Taamalli, A., Nsir, H., & Zarrouk, M. (2015). Olive tree (*Olea europeae* L.) leaves: Importance and advances in the analysis of phenolic compounds. *Antioxidants, 4*(4), 682–698.

Bellumori, M., Cecchi, L., Innocenti, M., Clodoveo, M. L., Corbo, F., & Mulinacci, N. (2019). The EFSA health claim on olive oil polyphenols: Acid hydrolysis validation and total hydroxytyrosol and tyrosol determination in Italian virgin olive oils. *Molecules, 24*(11), 2179.

Ben Mohamed, M., Rocchetti, G., Montesano, D., Ben Ali, S., Guasmi, F., Grati-Kamoun, N., et al. (2018). Discrimination of Tunisian and Italian extra-virgin olive oils according to their phenolic and sterolic fingerprints. *Food Research International, 106*, 920–927.

Bolger, A. M., Lohse, M., & Usadel, B. (2014). Trimmomatic: A flexible trimmer for Illumina Sequence Data. *Bioinformatics, btu170*.

Brodkorb, A., Egger, L., Alminger, M., et al. (2019). INFOGEST static *in vitro* simulation of gastrointestinal food digestion. *Nature Protocols, 14*, 991–1014.

Carrera-González, M. P., Ramírez-Expósito, M. J., Mayas, M. D., & Martínez-Martos, J. M. (2013). Protective role of oleuropein and its metabolite hydroxytyrosol on cancer. *Trends in Food Science & Technology, 31*(2), 92–99.

Caspi, R., Billington, R., Keseler, I. M., Kothari, A., Krummenacker, M., Midford, P. E., et al. (2020). The MetaCyc database of metabolic pathways and enzymes - a 2019 update. *Nucleic Acids Research, 48*(D1), D445–D453.

Clavel, T., Lepage, P., & Charrier, C. (2014). The family *Coriobacteriaceae*. In E. Rosenberg, E. F. DeLong, S. Lory, E. Stackebrandt, & F. Thompson (Eds.), *The Prokaryotes*. Berlin, Heidelberg: Springer. https://doi.org/10.1007/978-3-642-30138-4_343.

Dobrinčić, A., Repajić, M., Garofulić, I. E., Tuđen, L., Dragović-Uzelac, V., & Levaj, B. (2020). Comparison of different extraction methods for the recovery of olive leaves polyphenols. *Processes, 8*, 1008.

EFSA Journal. 9 (4) (2011), p. 2033, doi:10.2903/j.efsa.2011.2033, (25 pp.).

Farràs, M., Martinez-Gili, L., Portune, K., Arranz, S., Frost, G., Tondo, M., et al. (2020). Modulation of the gut microbiota by olive oil phenolic compounds: Implications for lipid metabolism, immune system, and obesity. *Nutrients, 12*(8), 2200.

Fernández-Reina, A., Urdiales, J. L., & Sánchez-Jiménez, F. (2018). What we know and what we need to know about aromatic and cationic biogenic amines in the gastrointestinal tract. *Foods, 7*(9), 145.

Ghisoni, S., Lucini, L., Angilletta, F., Rocchetti, G., Farinelli, D., Tombesi, S., et al. (2019). Discrimination of extra-virgin-olive oils from different cultivars and geographical origins by untargeted metabolomics. *Food Research International, 121*, 746–753.

González, E., Gómez-Caravaca, A. M., Giménez, B., Cebrián, R., Maqueda, M., Martínez-Férez, A., et al. (2019). Evolution of the phenolic compounds profile of olive leaf extract encapsulated by spray-drying during *in vitro* gastrointestinal digestion. *Food Chemistry, 279*, 40–48.

Heinritz, S. N., Mosenthin, R., & Weiss, E. (2013). Use of pigs as a potential model for research into dietary modulation of the human gut microbiota. *Nutrition Research Reviews, 26*, 191–209.

Jimenez-Lopez, C., Carpena, M., Lourenço-Lopes, C., Gallardo-Gomez, M., Lorenzo, J. M., Barba, F. J., et al. (2020). Bioactive compounds and quality of extra virgin olive oil. *Foods, 9*, 1014.

Kim, H. S., & Hur, S. J. (2018). Effect of *in vitro* human digestion on biogenic amine (tyramine) formation in various fermented sausages. *Journal of Food Protection, 81* (3), 365–368.

Liu, Z., Wang, N., Ma, Y., & Wen, D. (2019). Hydroxytyrosol improves obesity and insulin resistance by modulating gut microbiota in high-fat diet-induced obese mice. *Frontiers in Microbiology, 10*, 390.

Lobionda, S., Sittipo, P., Kwon, H. W., & Kyung Lee, Y. (2019). The role of gut microbiota in intestinal inflammation with respect to diet and extrinsic stressors. *Microorganisms, 7*(8), 271.

Martín-Vertedor, D., Garrido, M., Pariente, J. A., Espino, J., & Delgado-Adámez, J. (2016). Bioavailability of bioactive molecules from olive leaf extracts and its functional value. *Phytotherapy Research, 30*(7), 1172–1179.

Miceli, C., Santin, Y., Manzella, N., Coppini, R., Berti, A., Stefani, M., … Nediani, C. (2018). Oleuropein aglycone protects against MAO-A-induced autophagy impairment and cardiomyocyte death through activation of TFEB. *Oxidative Medicine and Cellular Longevity* (vol. 2018,, 13.

Minekus, M., Alminger, M., Alvito, P., et al. (2014). A standardised static in vitro digestion method suitable for food - An international consensus. *Food & Function, 5*, 1113–1124.

Miragoli, F., Patrone, V., Prandini, A., Sigolo, S., Dell'Anno, M., Rossi, L., et al. (2021). Implications of tributyrin on gut microbiota shifts related to performances of weaning piglets. *Microorganisms, 9*, 584.

Mosele, J. I., Martín-Pelàez, S., Macià, A., Farràs, M., Valls, R.-M., Catalàn, Ú., & Motilva, M.-J. (2014). Faecal microbial metabolism of olive oil phenolic compounds: *In vitro* and *in vivo* approaches. *Molecular Nutrition & Food Research, 58*(9), 1909-1819.

Nediani, C., Ruzzolini, J., Romani, A., & Calorini, L. (2019). Oleuropein, a bioactive compound from *Olea europaea* L., as a potential preventive and therapeutic agent in non-communicable diseases. *Antioxidants, 8*(12), 578.

Neis, E. P. J. G., Dejong, C. H. C., & Rensen, S. S. (2015). The role of microbial amino acid metabolism in host metabolism. *Nutrients, 7*(4), 2930–2946.

Paley, S., Parker, K., Spaulding, A., Tomb, J.-F., O'Maille, P., & Karp, P. D. (2017). The Omics Dashboard for interactive exploration of gene-expression data. *Nucleic Acids Research, 45*(21), 12113–12124.

Peršurić, Z., Saftic, L., Klisović, D., & Kraljević Pavelić, S. (2019). Polyphenol-based design of functional olive leaf infusions. *Food Technology & Biotechnology, 57*(2), 171–182.

Prieto, I., Hidalgo, M., Segarra, A. B., Martinez-Rodriguez, A. M., Cobo, A., Ramirez, M., et al. (2018). Influence of a diet enriched with virgin olive oil or butter on mouse gut microbiota and its correlation to physiological and biochemical parameters related to metabolic syndrome. *PLoS ONE, 13*, Article e0190368.

Rigacci, S., Guidotti, V., Bucciantini, M., Parri, M., Nediani, C., Cerbai, E., et al. (2010). Oleuropein aglycon prevents cytotoxic amyloid aggregation of human amylin. *The Journal of Nutritional Biochemistry, 21*(8), 726–735.

Rigacci, S., Miceli, C., Nediani, C., Berti, A., Cascella, R., Pantano, D., et al. (2015). Oleuropein aglycone induces autophagy via the AMPK/mTOR signalling pathway: A mechanistic insight. *Oncotarget, 6*(34), 35344–35357.

Rocchetti, G., Senizza, A., Gallo, A., Lucini, L., Giuberti, G., & Patrone, V. (2019). *In vitro* large intestine fermentation of gluten-free rice cookies containing alfalfa seed (*Medicago sativa* L.) flour: A combined metagenomic/metabolomic approach. *Food Research International, 120*, 312–321.

Rocchetti, G., Senizza, B., Giuberti, G., Montesano, D., Trevisan, M., & Lucini, L. (2020). Metabolomic study to evaluate the transformations of extra-virgin olive oil's antioxidant phytochemicals during *in vitro* gastrointestinal digestion. *Antioxidants, 9* (4), 302.

Rodríguez-Daza, M. C., Pulido-Mateos, E. C., Lupien-Meilleur, J., Guyonnet, D., Desjardins, Y., & Roy, D. (2021). Polyphenol-mediated gut microbiota modulation: Toward Prebiotics and further. *Frontiers. Nutrition, 8*, pages 347.

Romani, A., Campo, M., Urciuoli, S., Marrone, G., Noce, A., & Bernini, R. (2020). An industrial and sustainable platform for the production of bioactive micronized powders and extracts enriched in polyphenols from *Olea europaea* L. and *Vitis vinifera* L. wastes. *Frontiers Nutrition, 7*, 120.

Romani, A., Ieri, F., Urciuoli, S., Noce, A., Marrone, G., Nediani, C., et al. (2019). Health effects of phenolic compounds found in extra-virgin olive oil, by-products, and leaf of *Olea europaea L. Nutrients, 11*(8), 1776.

Rothwell, J. A., Pérez-Jiménez, J., Neveu, V., Medina-Ramon, A., M'Hiri, N., Garcia Lobato, P., … Scalbert, A. (2013). Phenol-Explorer 3.0: a major update of the Phenol-Explorer database to incorporate data on the effects of food processing on polyphenol content. *Database.* https://doi.org/10.1093/database/bat070

Roura, E., Koopmans, S. J., Lallèe, J. P., Le Huerou-Luron, I., de Jager, N., Schuurman, T., et al. (2016). Critical review evaluating the pig as a model for human nutritional physiology. *Nutrition Research Reviews, 29*, 60–90.

Ruzzolini, J., Peppicelli, S., Andreucci, E., Bianchini, F., Scardigli, A., Romani, A., et al. (2018). Oleuropein, the main polyphenol of *Olea europaea* leaf Extract, has an anti-cancer effect on human BRAF melanoma cells and potentiates the cytotoxicity of current chemotherapies. *Nutrients, 10*(12), 1950.

Ruzzolini, J., Peppicelli, S., Bianchini, F., Andreucci, E., Urciuoli, S., Romani, A., et al. (2020). Cancer glycolytic dependence as a new target of olive leaf extract. *Cancers, 12*(2), 317.

Salek, R. M., Steinbeck, C., Viant, M. R., Goodacre, R., & Dunn, W. B. (2013). The role of reporting standards for metabolite annotation and identification in metabolomic studies. *GigaScience, 2*(1), 2047-217X-2-13.

Santos, M. M., Piccirillo, C., Castro, P. M., Kalogerakis, N., & Pintado, M. E. (2012). Bioconversion of oleuropein to hydroxytyrosol by lactic acid bacteria. *World Journal of Microbiology and Biotechnology, 28*, 2435–2440.

Takahashi, S., Tomita, J., Nishioka, K., Hisada, T., & Nishijima, M. (2014). Development of a prokaryotic universal primer for simultaneous analysis of bacteria and archaea using next-generation sequencing. *PLoS ONE, 9*(8), Article e105592.

Williams, B. A., Bosch, M. W., Boer, H., Verstegenm, M. W. A., & Tamminga, S. (2005). An *in vitro* batch culture method to assess potential fermentability of feed ingredients for monogastric diets. *Animal Feed Science and Technology, 123–124*(Part 1), 445–462.